J. RADIAT. RES., 41, 213–226 (2000)

Hydrocephalus in Mice Following X-irradiation at Early Gestational Stage: Possibly Due to Persistent Deceleration of Cell Proliferation

HOSSAIN MD. AOLAD, MINORU INOUYE*, WIN DARMANTO, SHIZU HAYASAKA AND YOSHIHARU MURATA

Department of Teratology and Genetics, Research Institute of Environmental Medicine, Nagoya University, Nagoya 464–8601, Japan

(*Received, April 10, 2000*)
(*Revision received, June 13, 2000*)
(*Accepted, June 23, 2000*)

Brain abnormality/ Hydrocephalus/ Cell proliferation/ Early gestational stage/ Persistent effects

The pathogenesis of X-ray-induced congenital hydrocephalus was studied. Pregnant mice were irradiated at 1.4 Gy on gestational day 7 (G7). Four hours after irradiation, extensive cell death was evident in the neuroepithelium and underlying mesoderm of the head region, and proliferating cell nuclear antigen (PCNA)-immunoreactive cells almost disappeared. Embryos with thinner lamina terminalis of the telencephalon, when compared with that of the control, were found in the irradiated group on G9. As early as G11 in some irradiated embryos the telencephalic wall was thinner and lateral ventricles were larger than those of the control. The choroid invagination from the lamina terminalis began on G11 in the control brain, but not in the affected brain. During the following development, fetuses with readily apparent hydrocephalus were consistently found among irradiated fetuses. In these brains the brain mantle was thinner, the corpus striatum and thalamic regions were smaller, and lateral ventricles were larger than those of the control. Even on G11 and G13 the frequencies of PCNA-positive cells in the brain mantle and other brain regions were lower in the hydrocephalic brain than those of the control, suggesting a decelerated proliferation of successive cell generations following exposure to X-rays. The cerebral aqueduct was open in the hydrocephalic brain during the fetal period when the lateral ventricles were dilated. The head was vaulted after birth but the cerebral aqueduct was not completely occluded even in these animals. These findings suggested that cell death in the neuroepithelium followed by a persistent deceleration of neural cell proliferation, resulting in the hypoplasia of brain parenchyma with compensatory ventricular dilatation, is important for the establishment of hydrocephalus.

INTRODUCTION

Hydrocephalus is a malformation characterized by an abnormal accumulation of cerebrospinal fluid (CSF) in the cranial vault, accompanied by enlargement of the head and atrophy

*Corresponding author: Phone; +81–52–789–3874, Fax; +81–52–789–3876, E-mail; inouye@riem.nagoya-u.ac.jp

of the brain. Experimentally, congenital hydrocephalus has been induced by numerous insults such as radiation, infections, chemicals and nutritional deficiencies[1]. Based on histological examinations of fetuses and young animals, the pathogenesis of hydrocephalus has been repeatedly debated. The causes of hydrocephalus which have been proposed on the basis of various types of experiments are: stenosis or occlusion of the cerebral aqueduct[2–4], an overproduction or defective absorption of CSF[5], abnormal vascular formation in the brain mantle[6], increased permeability of the blood-brain barrier or blood-CSF barrier[7], and damage to the overlying brain parenchyma[8–11]. However, precise examinations of embryos to elucidate the primary causes of hydrocephalus have been difficult, because the incidences of hydrocephalus induced by teratogenic agents have been low in these experiments.

In our previous experiment, we attempted to obtain a high incidence of postnatally viable hydrocephalic offspring resulting from X-irradiation of pregnant mice, and determined the optimal conditions for this, i.e., 1.4 Gy as a radiation dose and gestational day 7 (G7) as an exposure time. The incidence of hydrocephalus in viable offspring was 46% under these conditions[12]. Hence, the method has provided a useful tool to observe the chronological development of hydrocephalus following exposure to X-radiation. Since X-ray doses can be exactly controlled, and the duration of radiation insults is very short, there is no concern about the influence of chemical retention or its metabolism which are unavoidable in cases of chemical teratogens.

In the present experiment we performed a chronological examination of mouse embryos from 4 h after X-ray exposure to adulthood. We found extensive apoptosis in the presumptive central nervous system as an acute effect of X-radiation. In addition, proliferation of neural cells in successive cell generations was decelerated, leading to the hypoplastic brain parenchyma. Such a persistent effect of X-radiation on successive cell generations of embryos was first demonstrated in the present study. The hypoplasia of the brain parenchyma and compensatory dilatation of cerebral ventricles might contribute to the development of hydrocephalus.

MATERIALS AND METHODS

Animals

Animals used were commercially supplied Slc:ICR mice. They were kept in an air-conditioned room (21 ± 1°C) with a relative humidity of 50 ± 10% under an alternating 12-h light/dark schedule. Food and water were provided ad libitum. Females 8 weeks of age or older were placed in cages with potent males. The occurrence of copulation was determined by the presence of vaginal plugs the next morning. The day when the plug was detected was designated as gestational day 0 (G0). During gestation the mice were housed individually. The present experiment was conducted under the Guidelines for Animal Experimentation, Nagoya University, on the basis of the Law Concerning the Protection and Control of Animals (law No. 105, 1973) of Japan.

X-irradiation

From the results of our preliminary experiment, the dose of X-irradiation and treatment day were determined to be 1.4 Gy and G7, respectively[12]. X-irradiation was performed with an X-ray apparatus SOFRON Model SVR-1505CDXII with radiation factors 140 kVp, 5 mA, 0.5 mm Al + 0.5 mm Cu filtration, and 104.0 ± 0.5 mGy/min exposure rate. To achieve a homogeneous dose distribution, the mice were put in individual plastic cages which were rotated at 4 rpm on a turntable during exposure. Control pregnant mice were treated in the same manner except for X-irradiation.

Evaluation of embryonic development

To study the developing brain of the fetuses, samples were collected every other day from G7, 4 h after exposure, through G19 (immediately before delivery). Pregnant mice were randomly assigned to different subgroups (3–7 litters in each group) for study on different days of gestation, and sacrificed by overdose of diethyl ether anesthesia. The fetuses were removed by uterine excision, and fixed in Bouin's solution overnight. There were a small number of fetuses with brain hernia and exencephaly in the irradiated group. Fetuses without these external malformations of the brain were embedded in paraffin, serially sectioned sagittally (G7) or frontally (G9-G19) at 5 μm thickness, and stained with hematoxylin and eosin (H&E) for microscopic examination.

The presence of apoptotic cells was assessed by the TUNEL [terminal deoxynucleotidyl transferase (TdT)-mediated dUTP-biotin nick end labeling] method 4 h after irradiation using TACS in situ apoptosis detection kit (Trivigen, Gaithersburg, MD, USA). The specimens were counterstained with methyl green.

Immunohistochemistry for proliferating cell nuclear antigen (PCNA)

Samples of five embryos in each group on G7, G11 and G13 were fixed in 4% paraformaldehyde overnight, then subsequently embedded in paraffin and sectioned at 5 μm thickness. Five sections from each embryo were unmasked by microwaves in 0.01 M citrate buffer (pH 6.0) at 80°C for 15 min followed by treatment with 0.006% pepsin (Sigma, St. Louis, MO, USA) digestion at 37°C for 15 min[13]. The sections were subsequently washed in phosphate buffered saline (PBS, pH 7.4) 5 times, and non-specific staining was blocked by incubating with 1% bovine serum albumin (BSA) in PBS and 0.01% NaN_3 for 30 min at room temperature. The sections were then incubated with monoclonal mouse anti-PCNA antibody (DAKO, Glostrup, Denmark) 1:200 in PBS with 0.2% BSA at 4°C overnight, washed in PBS 5 times and incubated further with biotinylated anti-mouse goat IgG secondary antibodies (1:50) in PBS for 1 h. Sections were again washed in PBS and incubated with horseradish peroxidase (HRP) streptavidine (1:50) in PBS for 1 h at room temperature. HRP reaction was developed at room temperature for 5 min in a solution of 5 mg of 3,3' -diaminobenzidine tetrachloride (Sigma) in 25 ml tris-buffered saline (pH 7.6) with 5 μl 30% H_2O_2. Samples incubated without anti-PCNA antibody served as a negative control.

Evaluation of postnatal development

Five control and 11 irradiated mice were allowed to give birth and, on the day of delivery, the number of neonates was counted. The live neonates were reared by their own dams and inspected everyday. From postnatal day 15 (P15) onward, a diagnosis of hydrocephalus was made according to the appearance of a dome-shaped head. A part of these results was already reported[12]. Hydrocephalic pups were deeply anesthetized with diethyl ether, perfused intracardially with 10% formalin and the brains were fixed with 10% formalin for 24 h. The samples were embedded in paraffin, serially sectioned in a frontal plane at 5 μm thickness and stained with H&E. Several sections through the cerebral aqueduct were chosen and immunostained with anti-glial fibrillary acidic protein (GFAP) antibody (DAKO, Glostrup, Denmark, diluted 1:500) using the same procedure as PCNA-immunostain, without microwave processing and pepsin digestion.

RESULTS

Embryonic development

The presumptive central nervous system of the embryo on G7 was composed of a pseudostratified epithelium, the neuroepithelium. The even alignment of the columnar cells with their large oval nuclei gave an ordered and regular appearance to the tissue as a whole (Fig. 1A,C). In all irradiated embryos examined at 4 h and 12 h after exposure on G7, dead cell debris was found in the amniotic cavity (Fig. 1B), and extensive cell death (40–60% in the midsagittal sections) was also evident in the neuroepithelium and underlying mesoderm of the head region (Fig. 1D). The disalignment of the cells imparted an irregular appearance to the tissue. A disruption in the surface of the neuroepithelium was observed (Fig. 1D). TUNEL-positive apoptotic cells were apparent in the neuroepithelium and mesoderm of the irradiated embryo 4 h after exposure (Fig. 1 inset).

By G9 the prosencephalon had cleaved laterally into two telencephalic vesicles both in the control and irradiated embryos. The lamina terminalis (the midline portion of the dorsal wall at the anterior region between the two telencephalic vesicles with a slight depression) was thinner in some irradiated embryos (five embryos out of eight examined) than that of the control (Fig. 2A,B). A single layer of neuroepithelial cells was observed in the region of the subnormal lamina terminalis in contrast to pseudostratified cuboidal cells in the control (Fig. 2A,B. insets).

On G11 the telencephalic wall in three out of seven irradiated embryos examined was thinner than that of the control. The lateral ventricles of these brains were dilated, and the corpus striatum and thalamic regions were also smaller when compared with those of the control (Fig. 2C,D). The choroid invagination began to develop from the lamina terminalis in the roof of the intraventricular foramen on this gestational day in the control (Fig. 2C), but no such rudiment of choroid plexus was seen in the subnormal brains (Fig. 2D).

By G13 in the control the corpus striatum and the thalamic regions had rapidly increased their volume. The choroid plexus was present both in the lateral ventricles (Fig. 3A) and in

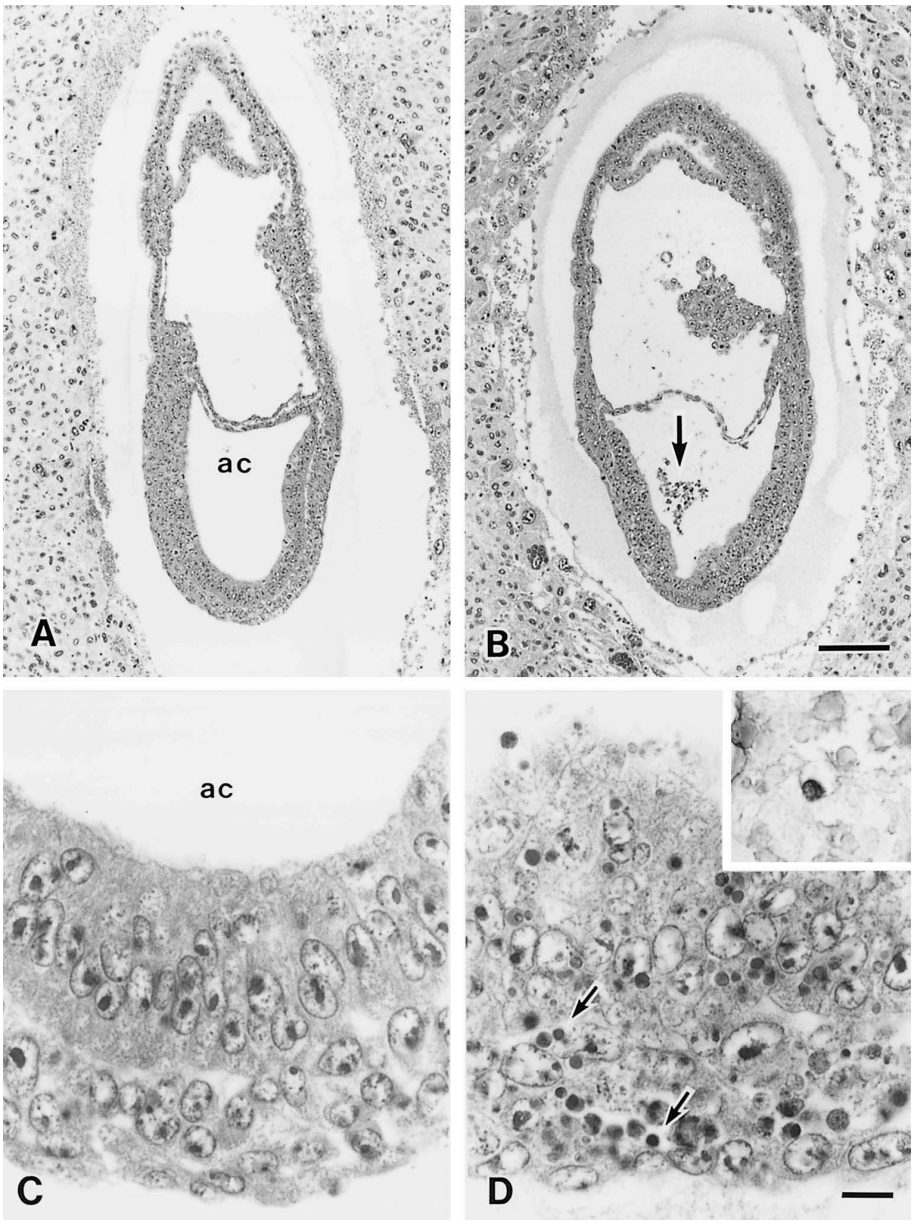

Fig. 1. (A) Sagittal section of the control embryo on G7 (ac, amiotic cavity). (B) Sagittal section of the embryo 4 h after exposure to X-radiation on G7, showing debris of dead cells (arrow) in the amniotic cavity. (C) High magnification of the neuroepithelium and underlying mesoderm in the head region of the control embryo (ac, amiotic cavity). (D) High magnification of the neuroepithelium and underlying mesoderm of the irradiated embryo, showing disruption of the surface of neuroepithelium and extensive cell death (arrows). H&E stain. A,B Bar = 50 μm and C,D Bar = 10 μm. Inset: Apoptotic cells in the neuroepithelium 4 h after exposure. TUNEL method.

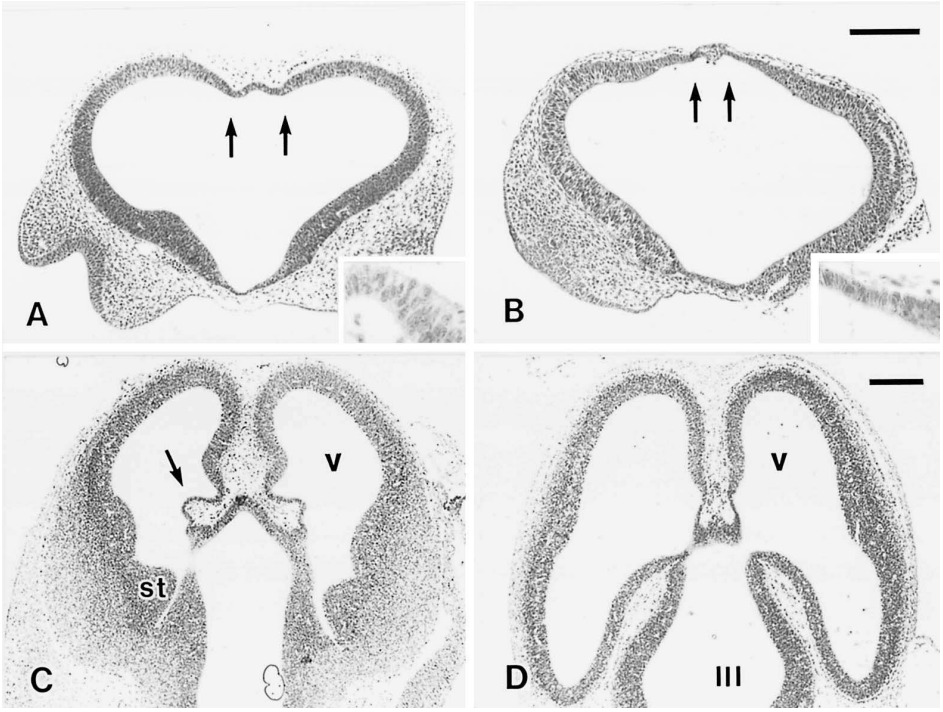

Fig. 2. (A) Frontal section through the lamina terminalis (between arrows) of the telencephalon of the control embryo on G9. Inset: High magnification of the lamina terminalis showing pseudostratified epithelium. (B) Frontal section of the irradiated embryo on G9 showing thinner lamina terminalis (between arrows) of the telencephalon than that of the control. Inset: High magnification of the lamina terminalis showing reduced thickness of the epithelium. (C) Frontal section of the control embryo on G11 showing the choroid invagination (arrow) from the lamina terminalis (st, corpus striatum; v, lateral ventricle). (D) Frontal section of the irradiated embryo on G11, in which the lateral (v) and third (III) ventricles are larger than those of the control. The choroid invagination is not seen. H&E stain. Bar = 200 μm.

the fourth ventricle. In some irradiated brains, hydrocephalus became apparent with dilated lateral and third ventricles. In such hydrocephalic embryos the brain mantle was thin, and the corpus striatum and thalamic regions were also small (Fig. 3B). The rudiments of choroid plexus appeared in this stage in the lateral ventricles. In hydrocephalic brains of G15 and G17, the cerebral mantle was strikingly thin, the corpus striatum and thalamic regions were small, the lateral and third ventricles were large, and the choroid plexus was shrunken (Fig. 3C-F).

Dilatation of the lateral ventricles became more marked in fetuses on G19 than in those sacrificed earlier in the irradiated group. At this stage the control brain showed slit-like lateral ventricles in close apposition between the brain mantle and hippocampus (Fig. 4A). In the hydrocephalic brain, a marked dilatation of the lateral and third ventricles was observed with a disrupted ventricular surface; the ependyma of the lateral ventricles appeared to be stretched and, in places, denuded (Fig. 4B). The hippocampus and thalamic regions were smaller in size, but lamination of the Ammon's horn and thalamic nuclei were discernible (Fig. 4B).

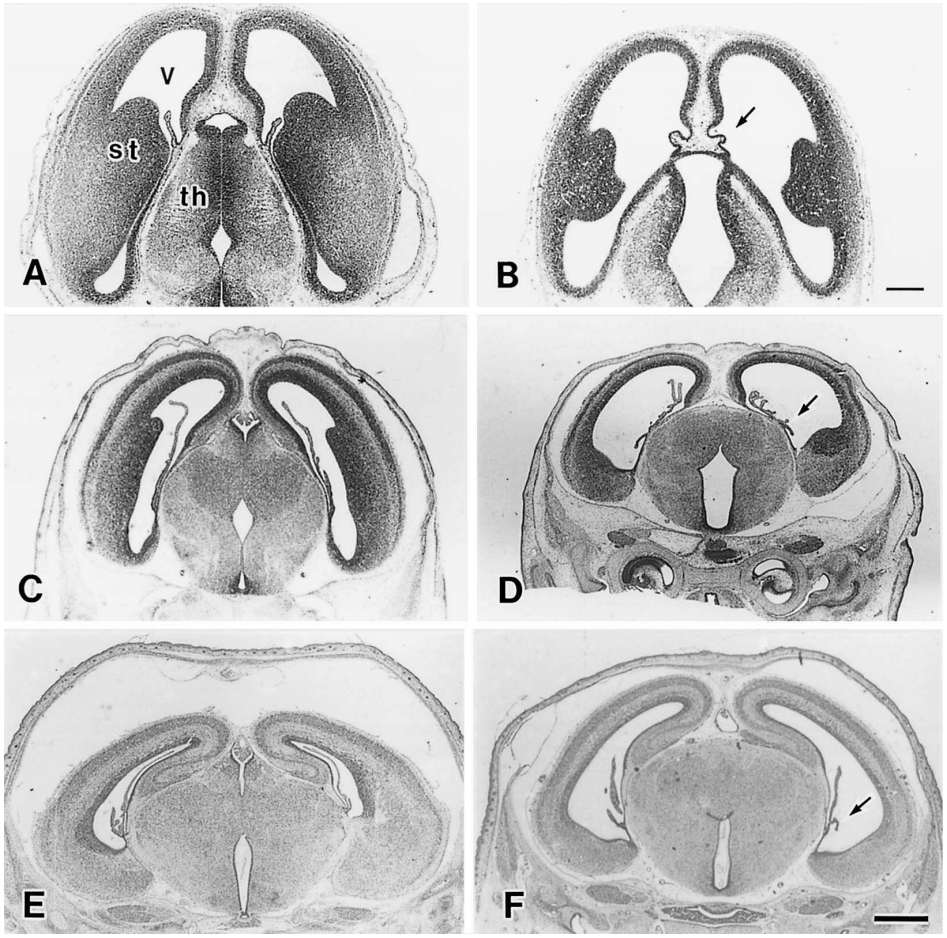

Fig. 3. (A),(C),(E) Frontal sections of the control brains on G13, G15 and G17, showing the development of the lateral ventricles (v), corpus striatum (st) and thalamus (th). (B) Frontal section of the hydrocephalic brain on G13 showing thin brain mantle, small corpus striatum and thalamus. The rudiment of choroid plexus (arrow) has appeared in the large lateral ventricles. (D),(F) Frontal sections of the hydrocephalic brains on G15 and G17, respectively, showing distended lateral ventricles with thinned parenchyma of the cerebral mantle, hypoplastic corpus striatum and thalamic regions, and shrunken choroid plexus (arrows). H&E stain. A,B Bar = 200 μm and C-F Bar = 1mm.

Although the brain mantle was thin in the hydrocephalic brain, four zones of the brain mantle, namely the marginal zone, cortical plate, intermediate zone and ventricular zone, could be distinguished (Fig. 4D).

To elucidate the mechanism behind the hypoplasia of parenchyma of the irradiated brain, we compared the proliferating activity of germinal cells along the cerebral ventricles between irradiated and control embryos by immunohistochemistry for proliferating cell nuclear antigen (PCNA). Four hours after exposure, PCNA-positive cells almost disappeared in the irradiated

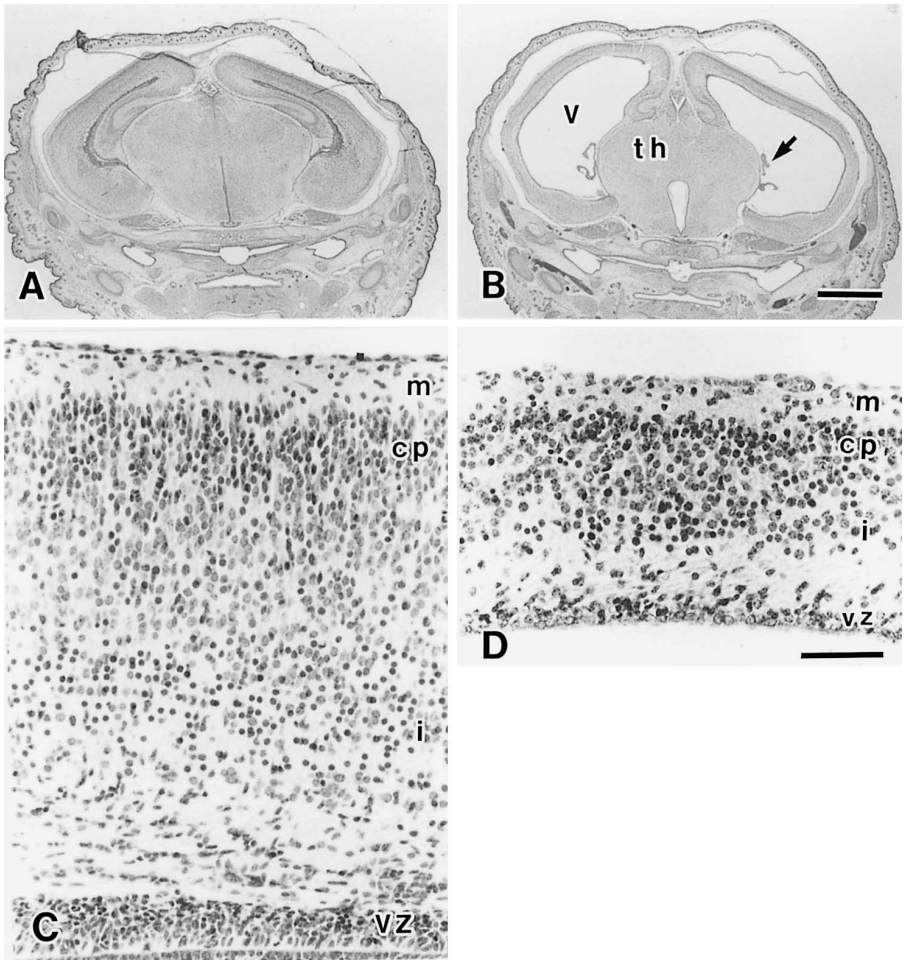

Fig. 4. (A) Frontal section of the control brain on G19 showing slit-like lateral ventricles with close apposition between the brain mantle and hippocampus. (B) Frontal section of the irradiated brain on G19 showing hydrocephalus with markedly enlarged lateral ventricles (v), thinned brain mantle, hypoplastic thalamus (th), and attenuated choroid plexus (arrow). (C) Frontal section of the control brain mantle on G19 showing marginal zone (m), cortical plate (cp), intermediate zone (i) and ventricular zone (vz). (D) Frontal section of the brain mantle of the hydrocephalic fetus showing its hypoplasia. H&E stain. A,B Bar = 200 μm and C,D Bar = 50 μm.

neuroepithelium, showing mitotic delay, while the majority of these cells were PCNA-positive in the control (Fig. 5A,B).

Both on G11 and G13 the reduced number of PCNA-positive cells was certainly observed in the whole brain areas examined, including the brain mantle, corpus striatum, thalamus and hypothalamus, in the subnormal brains of irradiated embryos. The number of positive cells in the parietal brain mantle was particularly reduced (Fig. 5E,F,I,J). Although the brain mantle was thinner in these brains, the population densities of cells stained with hematoxylin and eosin (H&E) were comparable between the control and subnormal brain tissue

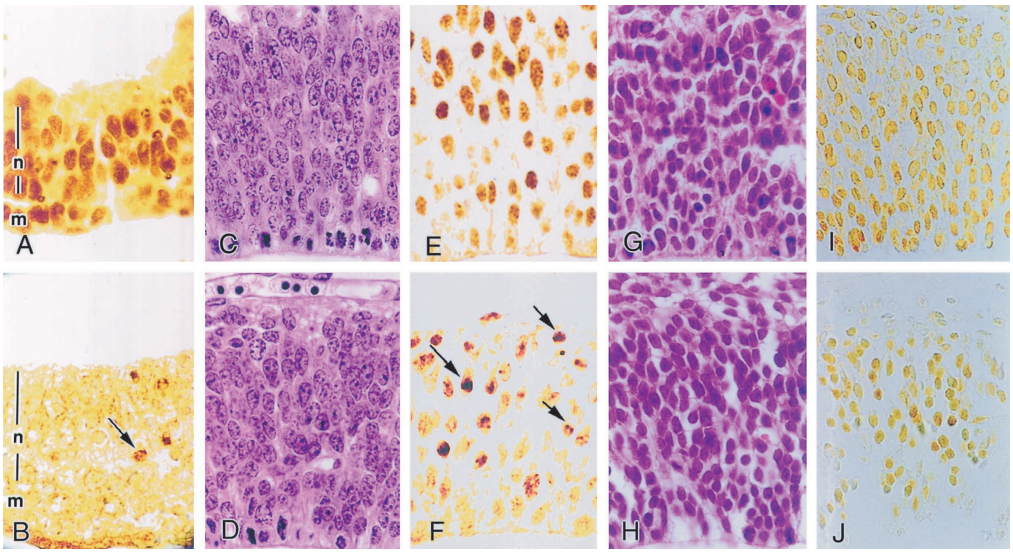

Fig. 5. (A) PCNA-immunostained sagittal section of the neuroepithelium (n) and underlying mesoderm (m) in the head region of the control embryo on G7, showing many PCNA-positive cells. (B) PCNA-immunostained sagittal section of the neuroepithelium (n) and underlying mesoderm (m) of the embryo 4 h after irradiation on G7, showing very few PCNA-positive cells (arrow). (C) H&E stained frontal section of the brain mantle of the control embryo on G11. (D) H&E stained frontal section of the brain mantle of the irradiated embryo on G11. Note the cell population density is similar to that of the control. (E) PCNA-immunostained frontal section of the brain mantle of the control embryo on G11. (F) PCNA-immunostained frontal section of the brain mantle of the irradiated embryo on G11. Note PCNA-positive cells (arrows) are fewer in number than those of the control. (G) H&E stained frontal section of the brain mantle of the control embryo on G13. (H) H&E stained frontal section of the brain mantle of the hydrocephalic embryo on G13. Note the cell population density is similar to that of the control. (I) PCNA-immunostained frontal section of the brain mantle of the control embryo on G13. (J) PCNA-immunostained frontal section of the brain mantle of the hydrocephalic embryo on G13. Note PCNA-positive cells are fewer than in the control.

at their corresponding stages (Fig. 5C,D,G,H).

Postnatal development

On postnatal day 0 (P0), no apparent differences between the irradiated and control offspring were found externally. By 2 weeks of age, development of a grossly apparent hydrocephalus with vaulted head was observed in irradiated offspring. As shown in Fig. 6, the autopsy of hydrocephalic animals revealed markedly dilated ventricles, attenuated choroid plexus, and thinned parenchyma of the brain. Even in severe hydrocephalus, the laminar formation of the cerebral cortex was distinguishable, but was considerably diminished in thickness when compared with the control (Fig. 6C). Paraventricular edema was observed, and the ependyma of the lateral ventricles appeared to be stretched and, in places, denuded (Fig. 6C).

Changes in cerebral aqueduct

We examined the cerebral aqueduct to study whether stenosis was the primary cause of

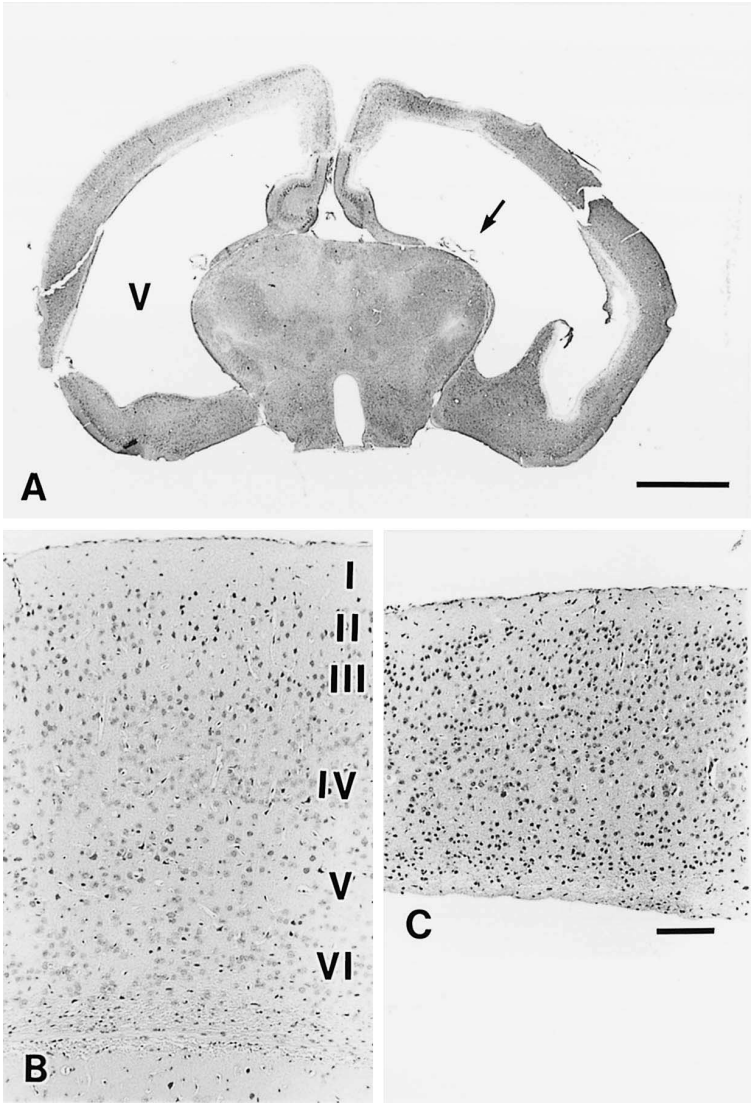

Fig. 6. (A) Frontal section of a severely hydrocephalic brain on P45, showing markedly dilated lateral ventricles (v), attenuated choroid plexus (arrow), and thinned parenchyma of the brain. (B) Frontal section of the cerebral cortex of the control adult brain. (C) Frontal section of the cerebral cortex of hydrocephalus. Lamination of the cerebral cortex is distinguishable, but considerably diminished in thickness. A Bar = 1 mm and B,C Bar = 100 μm.

X-ray-induced hydrocephalus. As shown in Fig. 7, serial frontal sections of the fetal brain revealed that the aqueduct was open in the hydrocephalic brains on G15, G17 and G19, although the lateral ventricles were markedly dilated at these stages. In adulthood the aqueducts of both control and hydrocephalic brains were narrow, and the lumen was slit-like in places. There was no evidence of complete occlusion of the aqueduct or inflammatory reac-

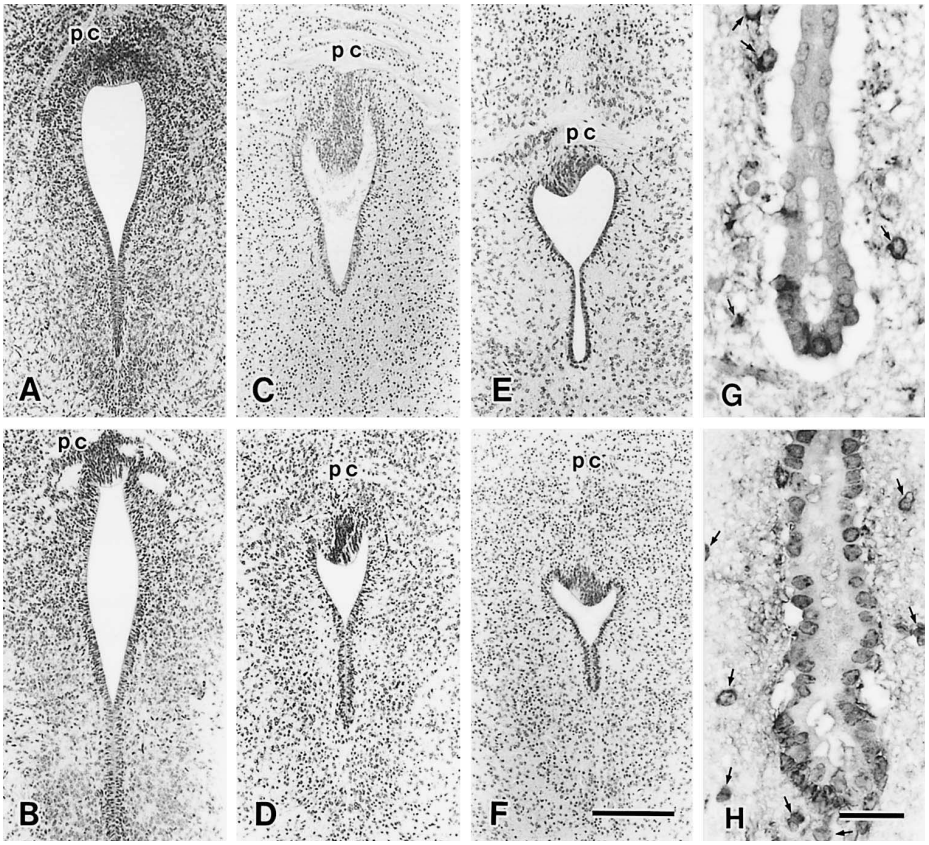

Fig. 7. (A),(C),(E) Frontal sections of the cerebral aqueduct of control fetuses on G15, G17, and G19, respectively (pc, caudal end of the posterior commissura). (B),(D),(F) Frontal sections of the cerebral aqueduct of hydrocephalic fetuses on G15, G17, and G19, respectively. Note the cerebral aqueduct is open during the fetal stage both in the control and hydrocephalic brains. H&E stain. Bar = 200 μm. (G),(H) Frontal sections of the cerebral aqueduct of the control and hydrocephalic brains, respectively, on P45. In the hydrocephalic brain, ependymal cells of the aqueduct are well preserved, and the lumen of the aqueduct is filled with a lightly stained material. Glial cells (arrows) in the tissue surrounding the aqueduct are not remarkably different in number between the control and hydrocephalic brains. GFAP-immunostain. Bar = 20 μm.

tion around it in the hydrocephalic brain. Although ependymal cells of the aqueduct were well preserved, the lumen of the aqueduct was filled with a lightly stained material (Fig. 7H). By the immunostaining of GFAP, there was no evidence of the glial cell proliferation in the surrounding tissue (Fig. 7G,H).

DISCUSSION

At the time of X-ray exposure in the present experiment, the mouse embryo was in the

neural plate stage of development. X-irradiation caused extensive apoptotic cell death in the neuroepithelium and underlying mesoderm of the head region. Despite this damage, the neural tube formation was completed in the majority of embryos. However, as early as G11, the first sign of hydrocephalus was detected: the telencephalic wall of some irradiated embryos was thinner than that of the control, though the telencephalon itself was similar in size. During the following development, fetuses with apparent hydrocephalus were consistently found among irradiated fetuses. In these brains the brain mantle was thinner, the corpus striatum and thalamic regions were smaller, and lateral ventricles were larger, than those of the control. These findings suggested that the hypoplasia of brain parenchyma with compensatory fluid accumulation in the cerebral ventricles was important for the establishment of X-ray-induced hydrocephalus.

Shortly after exposure to X-irradiation, PCNA-positive cells almost disappeared from the neuroepithelium of embryos. This showed the mitotic delay of surviving cells of the neuroepithelium, reflected by a known phenomenon, i.e., G_2-phase block caused by X-radiation[14], since the PCNA expression is involved in the DNA replication process[15,16]. Although PCNA is also involved in DNA repair, the immunoreaction is detected only in S-phase cells when conventional immunohistochemistry of formaldehyde-fixed specimens is employed[15–19]. If cells undergoing excision repair could also be stained with anti-PCNA antibody, we should have observed many PCNA-positive neuroepithelial cells 4 h after irradiation. This was not the case in our experiment (Fig. 5B).

Even four days (G11) and six days (G13) after exposure, a diminished number of PCNA-positive cells was observed in the hydrocephalic brain, particularly in the brain mantle, whereas the population density of cells was comparable between the control and hydrocephalic brains. Since the duration of M-phase is almost constant and that of S-phase is unlikely to be shortened by irradiation[20], the decreased frequency of cells in S-phase in the growing population reflects the elongated duration of either or both G_1- and G_2-phases. We therefore considered this finding represents a decelerated proliferation of cells. Although the mechanism of deceleration of cell proliferation in successive cell generations was not clear in the present experiment, ionizing radiation is known to have late and persistent effects[21,22]. These effects, observed in a variety of cells, include increased chromosomal aberrations, decrease in clone forming ability, and morphological abnormalities occurring de novo during successive cell generations following exposure[21,22]. The decelerated proliferation of successive generations of irradiated neuroepithelial cells is a new finding among the persistent effects of radiation. These results suggested that the deceleration of germinal cell proliferation, as well as the acute cell loss in the neuroepithelium after irradiation, is important with respect to the cause of hypoplasia of the brain parenchyma and compensatory ventricular dilatation. Similarly, in 6-aminonicotinamide-induced hydrocephalus, Chamberlain[8] observed reduced mitotic figures in the ventricular zone of the fetal brain until 6 days after maternal injection, and concluded that retarded neuroblast proliferation with compensatory fluid accumulation in cerebral ventricles was the origin of hydrocephalus.

Since cell death was also observed in the mesoderm of irradiated embryos, the possibility that mesodermal damage is another factor to induce hydrocephalus, cannot be dismissed. The

prechordal mesoderm is considered to have an inductive role in the morphogenesis of the forebrain, and its defect induces varying degrees of failure of the prosencephalon cleavage, holoprosencephaly[23]. Murakami et al.[24] irradiated pregnant mice on G8 and obtained fetuses with this type of malformation at a high frequency. However, in the present experiment, mice were irradiated on G7 and no fetuses suggesting failure of the cleavage of the presencephalon were detected. It will be of interest to investigate whether mesodermal defect contributes to the development of hydrocephalus.

In the present experiment, the cerebral aqueduct was open in the hydrocephalic fetuses on G15, G17 and G19 when the lateral ventricles were already markedly dilated. Accordingly, hydrocephalus observed in the present study is considered a communicating type. In adulthood the aqueduct was narrow and the lumen was slit-like in places both in the control and hydrocephalic brains. In the normal postnatal development of the brain, the cerebral aqueduct is reported to gradually decrease in size, probably compressed by the thickening of tissues immediately around the aqueduct as well as growing cerebral hemispheres[25]. The narrowing of the aqueduct is considered to be excessive if the lateral ventricles are distended[25]. In the present study, the hydrocephalic brain was not accompanied by the complete occlusion of the aqueduct. Although ependymal cells of the aqueduct were well preserved, the lumen of the aqueduct was filled with a lightly stained material. We did not examine the aqueduct with electron microscopy, however, the material was considered to be compacted cilia, which were observed in methylmercury-induced communicating hydrocephalus on postnatal day 20[10]. It is unclear in the present experiment whether the obstruction of the CSF flow occurred in postnatal life due to these changes.

In summary, exposure of mouse embryos to X-irradiation at the neural plate stage caused cell death in the neuroepithelium followed by persistent deceleration of neural cell proliferation. These events might contribute to the establishment of hydrocephalus with small brain parenchyma and compensatory dilatation of ventricles.

REFERENCES

1. Adeloye, A. and Warkany, J. (1976) Experimental congenital hydrocephalus. Child's Brain **2**: 325–360.
2. Dandy, W. E. (1920) The diagnosis and treatment of hydrocephalus resulting from strictures of the aqueduct of Sylvius. Surg. Gynecol. Obstet. **31**: 340–345.
3. Clark, F. H. (1934) Anatomical basis of hereditary hydrocephalus in the house mouse. Anat. Rec. **58**: 225–231.
4. Takeuchi, I. K. and Takeuchi, Y. K. (1986) Congenital hydrocephalus following X-irradiation of pregnant rats on an early gestational day. Neurobehav. Toxicol. Teratol. **8**: 143–150.
5. Kasubuchi, Y., Wakaizumi, S., Shimada, M. and Kusunoki, T. (1977) Cytosine arabinoside-induced transplacental dysgenetic hydrocephalus in mice. Teratology **16**: 63–70.
6. Kameyama, Y., Hayashi, Y. and Hoshino, K. (1972) Abnormal vascularity in the brain mantle with X-ray induced microcephaly in mice. Cong. Anom. **12**: 147–156.
7. Uno, M., Takano, T., Yamano, T. and Shimada, M. (1997) Tight junctional damage in experimental mumps-associated hydrocephalus. Cong. Anom. **37**: 157–163.
8. Chamberlain, J. G. (1970) Early neurovascular abnormalities underlying 6- aminonicotinamide (6-AN)-induced congenital hydrocephalus in rats. Teratology **3**: 377–388.

9. Kameyama, Y. and Hoshino, K. (1972) Postnatal manifestation of hydrocephalus in mice caused by prenatal X-radiation. Cong. Anom. **12**: 1–9.
10. Choi, B. H., Kim, R. C. and Peckham, N. H. (1988) Hydrocephalus following methylmercury poisoning. Acta Neuropathol. (Berl.) **75**: 325–330.
11. Inouye, M. and Kajiwara, Y. (1990) Strain difference of the mouse in manifestation of hydrocephalus following prenatal methylmercury exposure. Teratology **41**: 205–210.
12. Aolad, H. Md., Inouye, M., Hayasaka, S., Darmanto, W. and Murata, Y. (1998) High incidence of hydrocephalus following prenatal exposure to X-irradiation at early gestational stage in mice. Environ. Med. **42**: 60–63.
13. Ezaki, T. (1996) Antigen retrieval: its significance and drawbacks in immunohistochemistry. Acta Anat. Nippon. **71**: 615–628
14. Hawang, A. and Muschel, R. J. (1998) Radiation and the G_2 phase of the cell cycle. Radiat. Res. 150 (suppl.): S52–S59.
15. Bravo, R. and Macdonaldo-Bravo, H. (1984) Changes in the nuclear distribution of cyclin (PCNA) but not its synthesis depend on DNA replication. EMBO J. **4**: 655–661.
16. Bravo, R. (1986) Synthesis of the nuclear protein cyclin (PCNA) and its relationship with DNA replication. Exptl. Cell Res. **163**: 287–293.
17. Prelich, G., Kostura, M., Daniel, R., Mathews, M. B. and Stillman, B. (1987) The cell-cycle regulated proliferating cell nuclear antigen is required for SV40 DNA replication in vitro. Nature **326**: 471–473.
18. Miura, M. (1999) Detection of chromatin-bound PCNA in mammalian cells and its use to study DNA excision repair. J. Radiat. Res. **40**: 1–12.
19. LeCouter, J. E., Kablar, B., Whyte, P. F. M., Ying, C. and Rudnicki, M. A. (1998) Strain-dependent embryonic lethality in mice lacking the retinoblastoma-related p130 gene. Development **125**: 4669–4679.
20. Hoshino, K., Matsuzawa, T. and Murakami, U. (1973) Characteristics of the cell cycle of matrix cells in the mouse embryo during histogenesis of telencephalon. Exptl. Cell Res. **77**: 89–94.
21. Lambert, B., Holmberg, K., Hackman, P. and Wennborg, A. (1998). Radiation induced chromosomal instability in human T-lymphocytes. Mutat. Res. **405**: 161–70.
22. Roy, K., Kodama, S., Suzuki, K. and Watanabe, M. (1999) Delayed cell death, giant cell proliferation and chromosome instability induced by X-irradiation in human embryo cells. J. Radiat. Res. **40**: 311–322.
23. Smith, D. W. (1976) Holoprosencephaly anomalad. In: Recognizable Patterns of Human Malformation. Second Ed., pp. 366–367, W. B. Saunders, Philadelphia.
24. Murakami, U., Kameyama, Y., Majima, A. and Sakurai, T. (1962) Radiation malformations belonging to the cyclopia-arrhinencephalia-otocephalia group in the mouse foetus. J. Embryol. exp. Morph. **10**: 64–72.
25. Williams, B. (1973) Is aqueduct stenosis a result of hydrocephalus? Brain **96**: 399–412.